Extrinsic Noise Driven Phenotype Switching in a Self-Regulating Gene

Michael Assaf,[1] Elijah Roberts,[2] Zaida Luthey-Schulten,[3,4] and Nigel Goldenfeld[4]

[1]*Racah Institute of Physics, Hebrew University of Jerusalem, Jerusalem 91904, Israel*
[2]*Department of Biophysics, Johns Hopkins University, Baltimore, Maryland 21218, USA*
[3]*Department of Chemistry, University of Illinois at Urbana-Champaign, Urbana, Illinois 61801, USA*
[4]*Department of Physics and Center for the Physics of Living Cells, University of Illinois at Urbana-Champaign,
Urbana, Illinois 61801, USA*
(Received 11 February 2013; published 30 July 2013)

Analysis of complex gene regulation networks gives rise to a landscape of metastable phenotypic states for cells. Heterogeneity within a population arises due to infrequent noise-driven transitions of individual cells between nearby metastable states. While most previous works have focused on the role of intrinsic fluctuations in driving such transitions, in this Letter we investigate the role of extrinsic fluctuations. First, we develop an analytical framework to study the combined effect of intrinsic and extrinsic noise on a toy model of a Boolean regulated genetic switch. We then extend these ideas to a more biologically relevant model with a Hill-like regulatory function. Employing our theory and Monte Carlo simulations, we show that extrinsic noise can significantly alter the lifetimes of the phenotypic states and may fundamentally change the escape mechanism. Finally, our theory can be readily generalized to more complex decision making networks in biology.

Noise-driven switching between coexisting metastable states plays a key role in many systems in physics, chemistry, and biology [1–4]. Besides thermal or intrinsic noise (IN) that drives switching [5], such systems often experience extrinsic or environmental noise (EN) from the noisy environment or from being coupled to another fluctuating system [1]. Noise-driven escape from a metastable state while under the influence of EN has been previously studied in the context of population biology and population genetics (see, e.g., Refs. [6–8]), where it has been shown that, e.g., EN can drastically decrease the population's mean extinction time [7,8]. Moreover, recently there has been a large effort to predict the onset of EN-driven critical transitions and regime shifts in ecosystems (see, e.g., Ref. [9]).

In cellular biology, feedback-based gene regulatory networks have been shown to give rise to cellular phenotype (or epigenetic) landscapes with infrequent transitions of individual cells between multiple metastable states [10]. Driven by IN and EN [11], these transitions result in clonal populations of cells displaying multiple heritable phenotypes, whose coexistence, when stable over experimental time scales, can be considered a consequence of ergodicity breaking [12]. In developmental processes, the stability of the phenotypic states, quantified by the mean switching time (MST) to go from one state to another, is typically very long to ensure stable differentiation [13]. In microbial systems, however, MSTs that are no more than a few orders of magnitude longer than the cell cycle can provide a beneficial source of diversity in genetically identical populations. Such population heterogeneity has been proposed to give rise to a selective advantage via bet-hedging strategies, e.g., bacterial persistence [14].

Most previous studies of gene expression dynamics, including our own treatments [15], have focused on the role of IN (reviewed in Ref. [16]). Recently, however, gene expression under EN has also come under study [11,17,18]. Whereas IN is defined as the intracellular variability in identically regulated genes due to stochastic gene expression, EN is defined as intercellular variability due to fluctuations during gene expression that equally affect all genes within a cell. EN arises due to cell-to-cell variation in the numbers of ribosomes, RNA polymerases, and other key gene expression machinery, and variation in other slowly changing cellular parameters such as growth rate. EN has been shown to dominate variations in protein copy number, particularly above numbers of $\mathcal{O}(10)$ [18]. In studies of genetic switches, EN has been shown to induce bistability [19,20], vary the distribution tails [20], and modify switching times [21]. Yet, previous studies have not provided fundamental insight as to the interplay between IN and EN in the switching process, i.e., how the MSTs and switching paths deviate according to EN strength, correlation time, and statistics. Elucidating the relationship between IN and EN during switching is crucial to understanding how EN affects population heterogeneity in metastable systems.

In this Letter we study the combined influence of IN and EN on noise-driven switching in a simple bistable self-regulating gene (SRG) with positive feedback. We do so by casting the problem onto a set of coupled stochastic differential equations for the protein density and noise magnitude in the spirit of Ref. [2]. We then use a semiclassical treatment and Hamilton formulation to systematically study the effect of EN statistics, magnitude,

and correlation time on the switch's dynamics and, in particular, on the MSTs. We also study how EN affects the bistability range and escape mechanism of a system that is intrinsically noisy. All analytical results are corroborated by Monte Carlo (MC) simulations. Our analysis shows that the EN correlation time plays a key role in determining both the stability of the phenotypic state and the escape mechanism. This indicates that in biological systems, where the correlation time is thought to be long, phenotype switching may be driven primarily by EN.

Let $n(t)$ be the protein copy number and $N \gg 1$ be the protein abundance in the hi state. Proteins are produced at a rate $f(n)$, which is any Hill-like function to provide positive feedback, and decay with rate 1. We assume that proteins decay through dilution by cell division; thus time is measured in units of cell cycles. The mean protein density $\bar{x}(t) = \bar{n}(t)/N$ satisfies

$$\dot{\bar{x}} = f(\bar{x}) - \bar{x}. \qquad (1)$$

For simplicity we take $f(x) = \alpha_0 + (1 - \alpha_0)\theta(x - x_0)$, where $\theta(x)$ is the Heaviside step function, and $\alpha_0 < x_0 < 1$. Such a steplike regulatory function may be encountered, e.g., when multiple binding sites control a DNA transition between looped and unlooped regulatory states [22]. Equation (1) leads to a bistable system with three fixed points $x_1 < x_2 < x_3$, where $x_1 = \alpha_0$ and $x_3 = 1$ are attracting fixed points of the low and hi states respectively, while $x_2 = x_0$ is repelling. Typically, $\alpha_0 \ll 1$ so $x_3 \gg x_1$.

To model IN, we use the master equation (ME) for $P_n(t)$—the probability to find n proteins at time t: $\dot{P}_n = f(n-1)P_{n-1} + (n+1)P_{n+1} - [f(n) + n]P_n$. For simplicity we focus on the weak-noise regime $1 - x_0 \ll 1$, where (without loss of generality) the "switching barrier" between the hi and low states is small. Here, the ME is accurately approximated by the following Fokker-Planck equation (FPE) for the probability $P(x = n/N, t)$ [3,23]:

$$\partial_t P = -\partial_x\{[f(x) - x]P\} + 1/(2N)\partial_x^2\{[f(x) + x]P\}. \qquad (2)$$

Starting from the vicinity of the hi state, the system rapidly forms a quasistationary distribution (QSD) about the hi state, which slowly leaks through the unstable point $x = x_0$ [23–25]. In general, the metastable state decays as $P(x,t) \simeq \pi(x)e^{-t/\tau}$ where $\pi(x)$ is the QSD and τ is the MST. Employing the WKB ansatz $\pi(x) \sim e^{-NS(x)}$ for the QSD [24], where $S(x)$ is called the action function and $p_x(x) \equiv S'(x)$ is the momentum, in the leading order of $N \gg 1$, Eq. (2) gives rise to a stationary Hamilton-Jacobi equation (HJE):

$$H(x, p_x) = p_x[f(x) - x] + (p_x^2/2)[f(x) + x] = 0. \qquad (3)$$

Switching occurs along the zero-energy trajectory $p_x(x) = -2[f(x) - x]/[f(x) + x]$ of Eq. (3). For $x_0 < x \leq 1$, $p_x(x) = -2(1 - x)/(1 + x)$, which for $1 - x_0 \ll 1$ satisfies

$|p_x(x)| \ll 1$. This yields $S(x) = \int^x p_x(x')dx' = 2[x - 2\ln(1 + x)]$, and the QSD around $x = 1$: $\pi(x) \sim e^{-N[S(x) - S(1)]}$ with standard deviation $\sigma_{IN} \equiv N^{-1/2}$ due to IN. As $\tau_{hi \to low} \sim \pi(x_0)^{-1}$ [23,25], we thus have [26]

$$\ln \tau_{hi \to low} \simeq N[S(x_0) - S(1)] \simeq (N/2)(1 - x_0)^2 \equiv \Delta S_0, \qquad (4)$$

which is applicable as long as $\sigma_{IN} = N^{-1/2} \ll 1 - x_0$.

Next, we incorporate EN in the form of one or more fluctuating rates. We assume that cell-to-cell variability in transcription and translation rates causes, e.g., the protein production rate to fluctuate. In the hi state the production rate then becomes $1 + \xi(t)$, where $\xi(t)$ is fluctuating with finite correlation time. As we are interested in the hi → low transition we ignore fluctuations in α_0. We take $\xi(t)$ to be Ornstein-Uhlenbeck (OU) noise [3]: positively correlated Gaussian noise with zero mean, variance σ_{EX}^2, and correlation time τ_c, satisfying $\langle \xi(t)\xi(t') \rangle = \sigma_{EX}^2 e^{-|t-t'|/\tau_c}$. The OU process satisfies the following Langevin equation

$$\dot{\xi} = -\xi/\tau_c + \sqrt{2\sigma_{EX}^2/\tau_c}\,\eta(t), \qquad (5)$$

where η is white Gaussian noise, $\langle \eta(t)\eta(t') \rangle = \delta(t - t')$ [27]. Here, σ_{EX} and τ_c are characteristic of the environment and the cell's regulatory network and are generally unknown. Non-Gaussian statistics for EN have also been proposed [20], but further theoretical and experimental work is needed to uncover the source and form of EN.

To study the interplay between IN and EN, we combine Eq. (5) with the underlying IN dynamics [Eq. (2)]. Defining the fluctuating production rate $\tilde{f}(x, \xi) = \alpha_0 + (1 - \alpha_0 + \xi)\theta(x - x_0)$, drift term $A(x, \xi) = \tilde{f}(x, \xi) - x$, diffusion coefficient $B(x, \xi) = \tilde{f}(x, \xi) + x$, and the EN and IN variance ratio, $V \equiv \sigma_{EX}^2/\sigma_{IN}^2 = N\sigma_{EX}^2$, we obtain a 2D FPE for the joint probability $P(x, \xi, t)$ to find density x and noise magnitude ξ at time t [2,28,29]:

$$\partial_t P = -\partial_x\{A(x, \xi)P\} + \partial_\xi\{(\xi/\tau_c)P\}$$
$$+ 1/(2N)\partial_x^2\{B(x, \xi)P\} + 1/(2N)\partial_\xi^2\{(2V/\tau_c)P\}. \qquad (6)$$

Employing the WKB ansatz $\pi(x, \xi) \sim e^{-NS(x,\xi)}$ for the QSD, Eq. (6) yields a HJE: $H(x, \xi, p_x, p_\xi) = p_x A(x, \xi) - \xi p_\xi/\tau_c + (p_x^2/2)B(x, \xi) + p_\xi^2 V/\tau_c = 0$, with momenta $p_x \equiv \partial_x S$ and $p_\xi \equiv \partial_\xi S$. The HJE can be solved by considering the Hamilton equations $\dot{x}_i = \partial_{p_i}H$ and $\dot{p}_i = -\partial_{x_i}H$:

$$\dot{x} = A + p_x B, \qquad \dot{p}_x = -p_x[\partial_x A + (p_x/2)\partial_x B]$$
$$\ddot{\xi} \simeq \xi/\tau_c^2 - 2p_x V/\tau_c, \qquad (7)$$

where we have combined the equations for $\dot{\xi}$ and $\dot{p}_\xi$ to a single equation for $\ddot{\xi}$ and kept terms up to $\mathcal{O}(p_x) \ll 1$.

Equations (7) can be solved numerically for generic EN, which yields the corresponding action function
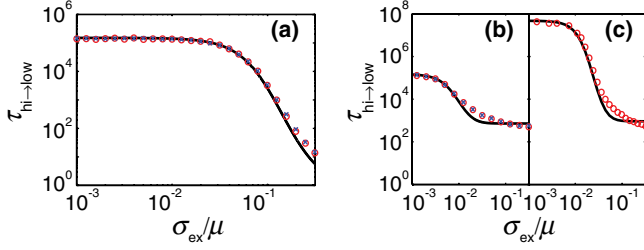
FIG. 1 (color online). $\tau_{\text{hi}\to\text{low}}$ versus the relative strength for white $\tau_c = 10^{-2}$ (a) and long-correlated $\tau_c = 10^3$ (b),(c) EN. MC simulations (the symbols) with noise in the production (circles) and decay (crosses) rates (that are indistinguishable) are compared with theory (lines): Eq. (8) (a) and Eq. (10) (b),(c). Here $N = 5000$, $\alpha_0 = 0.01$, and $x_0 = 0.93$ (a),(b) or $x_0 = 0.915$ (c). The values of $\tau_{\text{hi}\to\text{low}}$ are measured in units of cell cycles.

FIG. 2 (color online). $\tau_{\text{hi}\to\text{low}}$ as function of τ_c for various EN strengths: $\sigma_{\text{EX}}/\mu = 0.01$ (top left), 0.1 (top right), and 0.2 (bottom left). The lines are the analytical predictions of Eq. (8) (solid) and Eq. (10) (dotted). The lower right panel (see also inset) shows τ_c^{opt} versus EN strength: MC results (symbols) confirm the functional dependence on σ_{EX} predicted by Eq. (11) (line). Here $N = 5000$, $\alpha_0 = 0.01$, and $x_0 = 0.93$.

$S(x, \xi) = \int p_x(x, \xi) dx + p_\xi(x, \xi) d\xi$, and QSD. Analytical progress can be made in two limits: short-correlated white EN, $\tau_c \ll 1$, and long-correlated adiabatic EN, $\tau_c \gg 1$.

For white EN, we neglect $\ddot{\xi}$ in the third of Eqs. (7) [8], which yields $\xi \simeq 2 p_x V \tau_c < 0$ (see below). Substituting ξ into the first of Eqs. (7), we find for $x > x_0$: $\dot{x} = f(x) - x + 2 p_x V \tau_c + p_x [f(x) + x + 2 p_x V \tau_c]$, which originates from an effective white-noise Hamiltonian: $H \simeq p_x [f(x) - x] + (p_x^2/2)[f(x) + x + 2V\tau_c]$, where we have neglected $\mathcal{O}(p_x^3)$ terms. Solving $H = 0$, we find $p_x(x) = -2(1-x)/(1 + x + 2V\tau_c)$. This yields the MST in the white-EN regime:

$$\ln\tau_{\text{hi}\to\text{low}} \simeq \Delta S_0/(1 + V\tau_c), \qquad (8)$$

confirmed by MC simulations (see Figs. 1 and 2 and the Supplemental Material [30]). In Fig. 2 and below, μ denotes the QSD's average.

Now, to deal with long-correlated EN, we note that when $\tau_c \gg 1$, during the rare fluctuation that takes the system from the hi to the low state, the system samples an almost constant value of the noise $\xi = \xi_0$ [8]. For a constant ξ_0, the hi fixed point becomes $1 + \xi_0$. The optimal value of ξ_0 is found by minimizing the cost of switching given noise realization ξ_0, $\ln\tau_{\text{hi}\to\text{low}}(\xi_0) \simeq (N/2)(1 - x_0 + \xi_0)^2$, against the (absolute value of the) statistical weight of ξ, $N\xi_0^2/(2V)$. By doing so, we find $\xi^{\text{opt}} = -(1 - x_0)V/(1 + V)$, where $|\xi^{\text{opt}}| < 1 - x_0$ as expected. Plugging ξ^{opt} into $\tau_{\text{hi}\to\text{low}}(\xi_0)$ we find [31]

$$\ln\tau_{\text{hi}\to\text{low}} \simeq \Delta S_0 (1 + V)^{-2}. \qquad (9)$$

Equation (9) is valid for not too strong an EN, $V^2 \ll \Delta S_0$, which can only be satisfied when $\sigma_{\text{EX}} \ll 1 - x_0$.

In the opposite strong-EN regime $\sigma_{\text{EX}} \gtrsim 1 - x_0 \gg \sigma_{\text{IN}}$, it turns out that IN can be neglected, and the MST is governed by the mean time it takes the OU process to reach noise magnitude $\xi = x_0 - 1$ starting from $\xi = 0$ at $t = 0$. Here, for $\sigma_{\text{EX}} \gtrsim 1 - x_0$ we obtain that $\tau_{\text{hi}\to\text{low}} = \mathcal{O}(\tau_c)$ (see the Supplemental Material [30]).

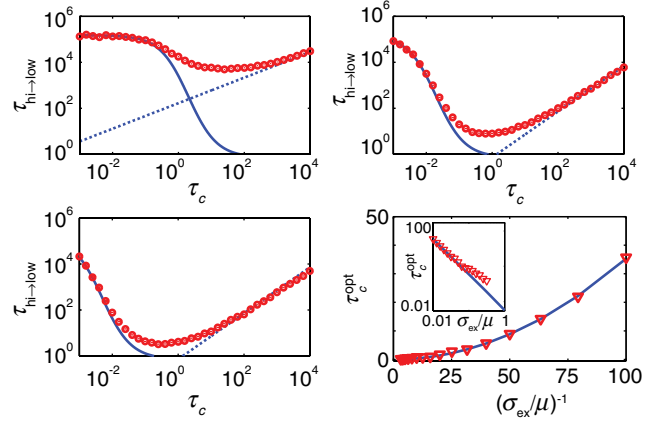This analysis gives rise to a correction in the adiabatic regime $\tau_c \gg 1$. Since $\ln\tau_{\text{hi}\to\text{low}} \simeq \ln\tau_c$ at $\sigma_{\text{EX}} \gtrsim 1 - x_0$, and $\ln\tau_{\text{hi}\to\text{low}} \simeq \Delta S_0$ at $\sigma_{\text{EX}} = 0$, Eq. (9) becomes

$$\ln\tau_{\text{hi}\to\text{low}} \simeq \ln\tau_c + (\Delta S_0 - \ln\tau_c)(1 + V)^{-2}, \qquad (10)$$

which compares well with MC results (see Figs. 1 and 2) [32].

Equations (8) and (10) show that EN of moderate strength can dramatically lower the MSTs, e.g., from 10^5 to ≤ 10 cell cycles (see Fig. 2). In microbial populations, where bet-hedging strategies require that heterogeneity develops relatively quickly, EN can therefore move the switching dynamics to biologically relevant time scales.

Figure 2 shows that for a given EN strength σ_{EX} there exists an optimal τ_c for which the MST is minimal. To evaluate τ_c^{opt} we add the white- and adiabatic-EN contributions [Eqs. (8) and (10)] for the MST, and differentiate the result with respect to τ_c. For $1 - x_0 \ll 1$, we find

$$\tau_c^{\text{opt}} \sim (1 - x_0)^2/\sigma_{\text{EX}}^2, \qquad (11)$$

whose dependence on σ_{EX} is confirmed by Fig. 2.

We also studied how EN affects bistability using the SRG model (1) with a more realistic Hill-type production rate

$$f(x) = \alpha_0 + (1 - \alpha_0)x^2/(x^2 + x_0^2). \qquad (12)$$

Noise-induced bistability has been studied in detail in the context of deterministic systems subject to external noise (see, e.g., Refs. [2]). Yet, here our underlying system is intrinsically noisy; given α_0 the system is bistable over a range of x_0 values [33]. Our aim is to investigate how adding EN alters the bistability region and mechanism of escape, as well as the effect of EN on the MSTs and the
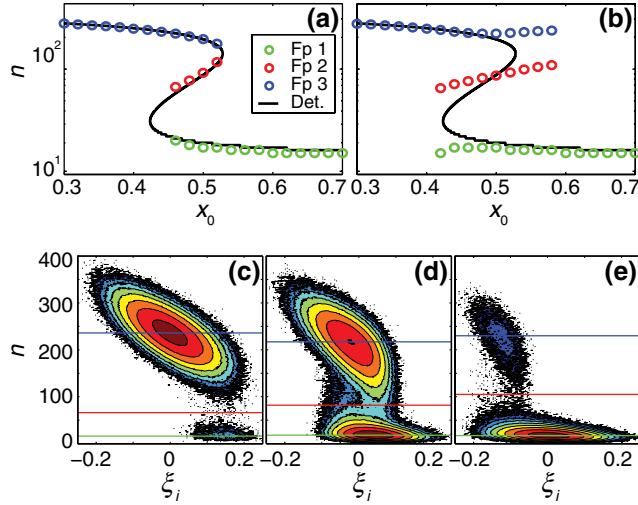
FIG. 3 (color online). (a),(b) The location of the stochastic fixed points of Eq. (1) with $f(x)$ given by Eq. (12), for EN with $\tau_c = 10^3$ and $\sigma_{EX}/\mu = 0.01$ (a) and $\sigma_{EX}/\mu = 0.05$ (b). The solid lines show the deterministic fixed points. (c)–(e) The steady-state 2D PDFs of finding protein number n and instantaneous EN magnitude ξ_i for $\sigma_{EX}/\mu = 0.05$ and $x_0 = 0.42$ (c), 0.48 (d), and 0.56 (e). Here $N = 300$, and $\alpha_0 = 0.05$.

FIG. 4 (color online). (a) $\tau_{\text{low}\to\text{hi}}$ and (b) $\tau_{\text{hi}\to\text{low}}$ for various EN strengths and $\tau_c = 10^3$. The population fraction P_{low} (c) and P_{hi} (d) in the low and hi states in steady state.

steady-state probability distribution functions (PDFs). To do so we ran MC simulations with a fluctuating decay rate $1 + \xi(t)$, to model cell-to-cell variability in the growth rate, and focused on adiabatic EN with $\tau_c = 10^3$.

To determine the influence of EN on the bistability range, we calculated the PDFs at various x_0 values from long-time simulations and extracted the position(s) of the sole maximum (monostable) or the two maxima separated by a minimum (bistable). These values we interpreted as stochastic equivalents to the deterministic fixed points. Our findings indicate that already for moderate EN strength $\sigma_{EX}/\mu = 0.05$, the locations of the stochastic fixed points strongly deviate from their deterministic locations [see Fig. 3(b)], which causes the range of x_0 over which the system is bistable to greatly increase. This effect becomes more pronounced as the EN strength further increases. For $\sigma_{EX}/\mu = 0.2$ the system was bistable over the entire range of x_0 sampled (0.3–0.7).

Furthermore (see the lower panels of Fig. 3), we calculated the 2D PDFs of finding protein number n and instantaneous fluctuation ξ_i. Figure 3(d) shows a case where the system is deterministically bistable. Here, for weak ξ_i the system undergoes IN-driven switching as expected. Yet, when the decay reaction is sampling the highest (lowest) rates due to EN, the system exists only in the low (hi) state and switches deterministically to the appropriate stable state. This effect appears in the 2D PDFs as two alternate switching paths: in the hi → low pathway $\xi_i > 0$, and in the low → hi pathway $\xi_i < 0$. Thus, the system's bistability is strongly affected by adiabatic EN driving the system between different
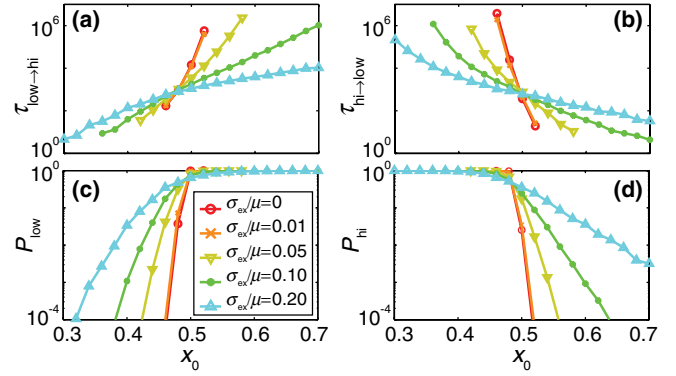
regions of parameter space with alternate fixed point configurations.

Figures 3(c) and 3(e) show the case where the system is deterministically monostable. When ξ_i is small one can see that the system behaves as though it has a single fixed point. However, when a large fluctuation occurs in the correct direction it can shift the system to a region of parameter space that is bistable. This effect gives rise to the increased bistability range observed in the simulations.

Finally, we calculated the MSTs for different EN strengths. The upper panels of Fig. 4 show that as the EN magnitude increases, the steepness of the curve versus x_0 is reduced for both $\tau_{\text{low}\to\text{hi}}$ and $\tau_{\text{hi}\to\text{low}}$. Such changes in the MSTs serve to make the less favorable state more populated across a wide range of x_0 values. This is illustrated in the lower panels of Fig. 4 showing the probability of the system being in the low or hi state: $P_{\text{low}} = \tau_{\text{hi}\to\text{low}}^{-1}/(\tau_{\text{hi}\to\text{low}}^{-1} + \tau_{\text{low}\to\text{hi}}^{-1})$ and $P_{\text{hi}} = 1 - P_{\text{low}}$. Here, as the EN magnitude is increased, not only does the bistability range expand but also the range at which the population is macroscopically heterogeneous (e.g., 1 part in 100). Furthermore, the probability tails decrease much slower than a system with only IN, which may explain experimental observations of cells persisting in lowly populated phenotypes across unexpected conditions.

Our theoretical results can be readily generalized to more complex higher-dimensional models of cellular decision making where, in addition, EN is present in multiple kinetic rates. Importantly, due to a lack of experimental data regarding the EN properties, our theory may allow to deconvolute the effects of IN and EN on switching from switching trajectories of individual cells subject to EN.

[1] W. Horsthemke and R. Lefever, *Noise-Induced Transitions: Theory and Application in Physics, Chemistry, and Biology* (Springer-Verlag, Berlin, Germany, 1984).

[2] P. Hänggi, P. Talkner, and M. Borkovec, Rev. Mod. Phys. **62**, 251 (1990); P. Hänggi and P. Jung, Adv. Chem. Phys. **89**, 239 (1995).

[3] C. W. Gardiner, *Handbook of Stochastic Methods for Physics, Chemistry and the Natural Sciences* (Springer, New York, 2004).

[4] G. Balázsi, A. van Oudenaarden, and J. J. Collins, Cell **144**, 910 (2011); I. Golding, Annu. Rev. Biophys. **40**, 63 (2011).

[5] J. Hasty, J. Pradines, M. Dolnik, and J. J. Collins, Proc. Natl. Acad. Sci. U.S.A. **97**, 2075 (2000); T. B. Kepler and T. C. Elston, Biophys. J. **81**, 3116 (2001); E. Aurell and K. Sneppen, Phys. Rev. Lett. **88**, 048101 (2002); A. M. Walczak, J. N. Onuchic, and P. G. Wolynes, Proc. Natl. Acad. Sci. U.S.A. **102**, 18926 (2005); M. J. Morelli, R. J. Allen, S. Tănase-Nicola, and P. R. ten Wolde, J. Chem. Phys. **128**, 045105 (2008); N. Chia, I. Golding, and N. Goldenfeld, Phys. Rev. E **80**, 030901(R) (2009); J. Wang, K. Zhang, and E. Wang, J. Chem. Phys. **133**, 125103 (2010).

[6] S. Karlin and B. Levikson, Theor. Popul. Biol. **6**, 383 (1974); J. F. Crow and M. Kimura, *An Introduction to Population Genetics Theory* (Harper & Row, New York, 1970).

[7] E. G. Leigh, J. Theor. Biol. **90**, 213 (1981); R. Lande, Am. Nat. **142**, 911 (1993); K. Johst and C. Wissel, Theor. Popul. Biol. **52**, 91 (1997).

[8] A. Kamenev, B. Meerson, and B. Shklovskii, Phys. Rev. Lett. **101**, 268103 (2008), and references therein.

[9] M. Scheffer, S. Carpenter, J. A. Foley, C. Folke, and B. Walker, Nature (London) **413**, 591 (2001); M. Scheffer, J. Bascompte, W. A. Brock, V. Brovkin, S. R. Carpenter, V. Dakos, H. Held, E. H. van Nes, M. Rietkerk, and G. Sugihara, Nature (London) **461**, 53 (2009).

[10] H. H. Chang, P. Y. Oh, D. E. Ingber, and S. Huang, BMC Cell Biol. **7**, 11 (2006); W. K. Smits, O. P. Kuipers, and J. Veening, Nat. Rev. Microbiol. **4**, 259 (2006).

[11] M. B. Elowitz, A. J. Levine, E. D. Siggia, and P. S. Swain, Science **297**, 1183 (2002).

[12] J. Garcia-Ojalvo and A. M. Arias, Curr. Opin. Genet. Dev. **22**, 619 (2012); A. Rocco, A. M. Kierzek, and J. McFadden, PLoS One **8**, e54272 (2013).

[13] S. Huang, Development (Cambridge, U.K.) **136**, 3853 (2009).

[14] N. Q. Balaban, J. Merrin, R. Chait, L. Kowalik, and S. Leibler, Science **305**, 1622 (2004).

[15] M. Assaf, E. Roberts, and Z. Luthey-Schulten, Phys. Rev. Lett. **106**, 248102 (2011); E. Roberts, A. Magis, J. O. Ortiz, W. Baumeister, and Z. Luthey-Schulten, PLoS Comput. Biol. **7**, e1002010 (2011); T. M. Earnest, E. Roberts, M. Assaf, K. Dahmen, and Z. Luthey-Schulten, Phys. Biol. **10**, 026002 (2013).

[16] M. Kaern, T. C. Elston, W. J. Blake, and J. J. Collins, Nat. Rev. Genet. **6**, 451 (2005); A. Eldar and M. B. Elowitz, Nature (London) **467**, 167 (2010); B. Munsky, G. Neuert, and A. van Oudenaarden, Science **336**, 183 (2012).

[17] P. S. Swain, M. B. Elowitz, and E. D. Siggia, Proc. Natl. Acad. Sci. U.S.A. **99**, 12 795 (2002); J. Paulsson, Nature (London) **427**, 415 (2004); J. M. Pedraza and A. van Oudenaarden, Science **307**, 1965 (2005); M. Scott, B. Ingalls, and M. Kaern, Chaos **16**, 026107 (2006); D. Volfson, J. Marciniak, W. J. Blake, N. Ostroff, L. S. Tsimring, and J. Hasty, Nature (London) **439**, 861 (2006); A. Hilfinger and J. Paulsson, Proc. Natl. Acad. Sci. U.S.A. **108**, 12 167 (2011).

[18] J. R. S. Newman, S. Ghaemmaghami, J. Ihmels, D. K. Breslow, M. Noble, J. L. DeRisi, and J. S. Weissman, Nature (London) **441**, 840 (2006); Y. Taniguchi, P. J. Choi, G.-W. Li, H. Chen, M. Babu, J. Hearn, A. Emili, and X. S. Xie, Science **329**, 533 (2010).

[19] M. Samoilov, S. Plyasunov, and A. P. Arkin, Proc. Natl. Acad. Sci. U.S.A. **102**, 2310 (2005); M. Leisner, J.-T. Kuhr, J. O. Rädler, E. Frey, and B. Maier, Biophys. J. **96**, 1178 (2009); T. L. To and N. Maheshri, Science **327**, 1142 (2010).

[20] V. Shahrezaei, J. F. Ollivier, and P. S. Swain, Mol. Syst. Biol. **4**, 196 (2008).

[21] B. Hu, D. A. Kessler, W.-J. Rappel, and H. Levine, Phys. Rev. Lett. **107**, 148101 (2011).

[22] J. M. G. Vilar and L. Saiz, Phys. Rev. Lett. **96**, 238103 (2006).

[23] C. Escudero and A. Kamenev, Phys. Rev. E **79**, 041149 (2009); M. Assaf and B. Meerson, Phys. Rev. E **81**, 021116 (2010).

[24] A. D. Wentzell and M. I. Freidlin, Russ. Math. Surv. **25**, 1 (1970); M. I. Dykman, E. Mori, J. Ross, and P. M. Hunt, J. Chem. Phys. **100**, 5735 (1994).

[25] M. Assaf and B. Meerson, Phys. Rev. Lett. **97**, 200602 (2006); Phys. Rev. E **75**, 031122 (2007).

[26] The MST can be exactly found here, since the underlying master equation involves only single-step processes [3].

[27] In the Langevin equation (5) $\eta(t)$ can be defined as the $dt \to 0$ limit of the temporally uncorrelated normal random variable with mean 0 and variance $1/dt$.

[28] Here we have increased the problem's dimensions from 1 to 2 by considering the noise magnitude as an effective additional species and coupling it to the protein species.

[29] E. Y. Levine and B. Meerson, Phys. Rev. E **87**, 032127 (2013).

[30] See Supplemental Material at http://link.aps.org/supplemental/10.1103/PhysRevLett.111.058102 for supplementary results and details on the numerical methods.

[31] This result can be equivalently obtained by integrating over $\tau_{\mathrm{hi}\to\mathrm{low}}^{-1}(\xi_0) \sim e^{-(N/2)(1-x_0+\xi_0)^2}$, with the Gaussian weight $e^{-N\xi_0^2/(2V)}$ of ξ_0. Using the saddle-point approximation, we recover ξ^{opt} and, consequently, Eq. (9).

[32] We have repeated the derivations using a fluctuating decay rate: $1 + \xi(t)$. For $1 - x_0 \ll 1$, the MST results coincide with Eqs. (8) and (9) (see Fig. 1 and the Supplemental Material [30]).

[33] Here x_0 can be interpreted as an environmental input, e.g., the concentration of an inducer or antibiotic.